ACERP: Vol. 1, No. 3, (Autumn 2015) 22-27

Advanced Ceramics Progress

Research Article

Journal Homepage: www.acerp.ir

# Microstructured and Magnetic Properties of $Sr_2Co_{1.7}Mg_{0.3}Fe_{11.2}Sn_{0.4}Zn_{0.4}O_{22}$ Hexaferrite Synthesized by Auto-Combustion Sol-Gel Metho

**A. Jafari *[a], A. Honarbakhsh Rauof [a], O. Mirzaee[a], Y. Alizad Farzin[b]**

[a] *Faculty of Materials Engineering and metallurgy, Semnan University, Semnan, Iran.*
[b] *School of Metallurgy and Materials Engineering, College of Engineering, University of Tehran, P.O. Box 14395-553, Tehran, Iran.*

*PAPER INFO*

*Paper history:*
Received 27 June 2015
Accepted in revised form 14 February 2016

*Keywords*:
Y-type hexaferrite
Sol-gel auto combustion
Magnetic properties
Calcination temperature

*ABSTRACT*

A single phase Y-type hexagonal ferrite $Sr_2Co_{1.7}Mg_{0.3}Fe_{11.2}Sn_{0.4}Zn_{0.4}O_{22}$ was synthesized by sol–gel auto combustion method. The microstructured and magnetic properties of this Y-type hexagonal ferrite composition have been investigated. Different experimental techniques such as differential thermal and thermo-gravimetric analyses, X-ray diffraction, Fourier transform infrared spectroscopy, high resolution field emission scanning electron microscopy and vibrating sample magnetometry were used to investigate the sample. The X-ray diffraction (XRD) patterns confirm single phase Y-type hexagonal ferrite powders were obtained after calcinations at 1000 °C and showed that the crystallite size is 44 nm. The microstructures of the pure powders appeared as a hexagonal platelet-like structure and particles size was 90-210 nm .The saturation magnetization ($M_s$) and the coercivity ($H_c$) of the samples were in the range, 28.34–48.47 emu/g and 637-1108 Oe, respectively. The heat treatment temperature increased the magnetization, following a decrease in coercivity due to intermediate phases replacement by single Y-type hexaferrite, Which can be used as soft magnetic materials in multilayer inductors for high frequency applications.

## 1. INTRODUCTION

Ferrites have continued to attract attention over years. As magnetic materials, ferrites cannot be replaced by any other magnetic materials because they are relatively inexpensive and have high Curie temperature, coercive force and magnetic anisotropy field, excellent chemical stability, corrosion resistivity and wide range of technological applications in transformer core [1-3]. Hexaferrites have been classified according to their structure and chemical composition into six main classes: M-type or $AFe_{12}O_{19}$, Y-type or $A_2Me_2Fe_{12}O_{22}$, W-type or $AMe_2Fe_{16}O_{27}$, Z-type or $A_3Me_2Fe_{24}O_{41}$, X-type or $A_2Me_2Fe_{28}O_{46}$ and U-type or $A_4Me_2Fe_{36}O_{60}$, where Me represents a divalent ion from the first transition series and A represents $Sr^{2+}$, $Ba^{2+}$ and $Pb^{2+}$ ions of the same ionic radii as the oxygen ions and therefore can replace them in the lattice [4, 5]. Synthesis method of Y-type hexaferrite strongly determines its homogeneity, particle size and shape, and magnetic characteristics [3]. The sol–gel technique is receiving much more attention because it can be applied to prepare an extremely wide variety of materials. This technique also offers the possibility of controlling the size and distribution of particles and also their shapes [6, 5]. In this manuscript, we describe the preparation of the novel $Co_2Y$ type hexaferrite by auto combustion sol–gel method and evaluation of their formation process, microstructured and magnetic properties as a function of calcination temperature.

## 2. MATERIALS AND METHODS

### 2.1. PRODUCING HEXAFERRITE POWDER

The required amount of starting materials i.e. $Sr(NO_3)_2$, $Co(NO_3)_2.6H_2O$, $Fe(NO_3)_3.9H_2O$, $SnCl_4.5H_2O$, $Mg(NO_3)_2.6H_2O$ and $Zn(NO_3)_2.6H_2O$ for the composition were taken according to stoichiometric ratios. Citric acid was used as a chelating agent for homogenous, steady and transparent sol solution and as a fuel for its complexion ability, low ignition temperature

*Corresponding Author's Email: a.jafari@semnan.ac.ir.

(i.e. 200–250 ˚C) and controlled combustion reaction with nitrates compared to other types of fuels [7]. Metal nitrates and citric acid were dissolved in 400 ml of deionized water to form aqueous solutions with a continuous magnetic stirring at 40 ˚C for 4hrs. The pH value at 7 was maintained by using ammonia solution at room temperature, and continued to stirred under the temperature of 80 ˚C, at this temperature evaporation of deionized water started and after complete evaporation, auto combustion process would be started. The reaction continued and gel converted into ash following auto-combustion was done [2], as it is shown in Figure 1. The dried gel was exposed to 450 ˚C for an hour in order to decompose citric acid completely [7] and subsequently calcined in the air at 800, 900, 950, 1000 and 1050 ˚C for 3hrs using a heating rate of 5 ˚C/min.

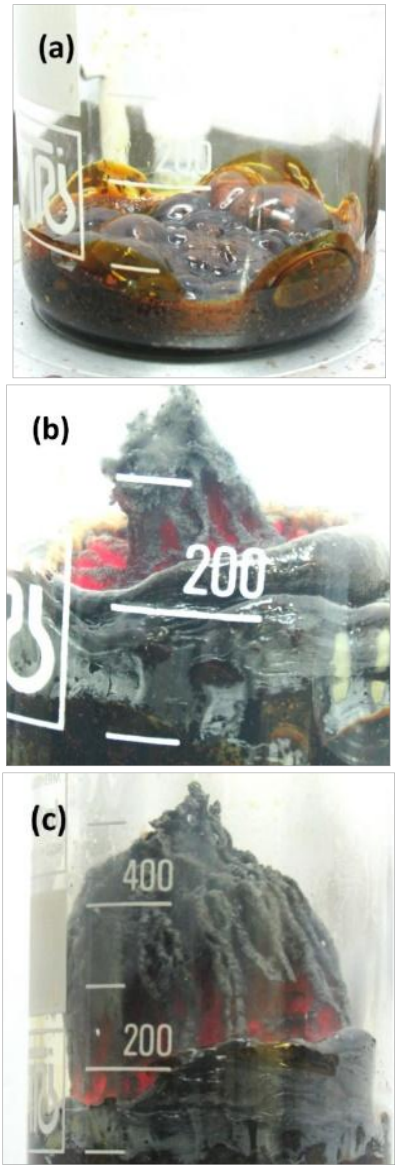


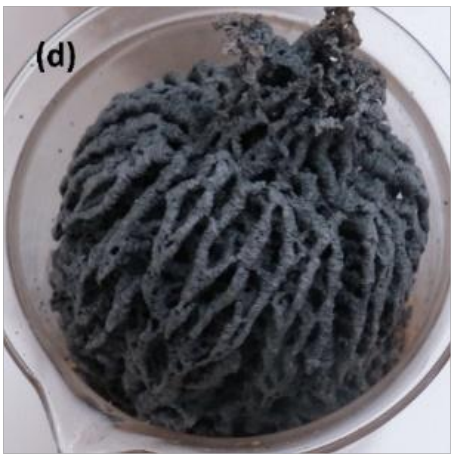


**Figure 1.** (a): Gelation, (b): initiation, (c); the auto-combustion process, and (d): the burnt and porous product of Y-type precursor synthesized via sol-gel auto-combustion method.

## 2.2. CHARACTERIZATION

The thermal decomposition behavior of the precursor was investigated by thermo-gravimetric and differential thermal analysis (TGA–DTA) at a heating rate of 10 ˚C.min$^{-1}$ in air on the Linseis (model L81). The crystalline phase structure was determined by Bruker D8 Advance X-ray diffractometer (XRD) using CuKα radiation. Average crystallite sizes (D) were determined from the XRD peaks using Scherrer's formula (Eq. 1),

$$D = \frac{k\lambda}{\beta \cos\theta} \quad (1)$$

where k is the shape coefficient (value between 0.9 and 1.0), λ is the wavelength, β is the full width at half maximum (FWHM) of each phase and θ is the diffraction angle.

Lattice constants (a and c) and volume of unit cell (V) for each sample was calculated based on the following formula [14].

$$d_{hkl} = \left(\frac{4}{3}\frac{h^2 + hk + k^2}{a^2} + \frac{l^2}{c^2}\right)^{-\frac{1}{2}} \quad (2)$$

$$V = a^2 c \sin\theta \quad (3)$$

Where λ is the wavelength, 2θ is between 10-90 degree, a and c are the lattice constants and hkl are the corresponding Miller indices [7, 10, 16]. Fourier transform infrared spectroscopy (FT-IR) spectra of KBr powder-pressed pellets were recorded on a BRUKER VECTOR 22 spectrometer. Morphology of the particles was investigated by MIRA3 TESCAN high resolution field emission scanning electron microscopy (FESEM). Magnetic properties of all samples were investigated by

a vibrating sample magnetometer (VSM) with the maximum applied field of 10 kOe at room temperature.

## 3. RESULT AND DISCUSSION

### 3.1. TG AND DTA ANALYSIS

The TGA and the DTA curves of as-burnt powder sample in the range of 25–1200 ˚C are shown in Figure 2. The first weight loss observed below 200 ˚C (i) could be attributed to the evaporation of residual water present in the sample. The weight loss of about 300-500 ˚C limited area (ii) resulted from the decomposition of C–H organic components and amino group. The strong weight loss of region from 650 to 750 ˚C (iii) was related to the complete decomposition of the carboxyl metal and nitrate groups [8]. No additional weight loss was observed at temperature above 1000 ˚C (iv), which implied the complete decomposition of organic components and the formation of metal oxides. The exothermic peaks at about 400 ˚C correspond to the formation of oxides from hydroxide [4]. The DTA curve fluctuation in the region above 1000 ˚C and no corresponding weight loss in the TGA curve implied the existence of complicated phase transition between the new-produced metal oxides [9].

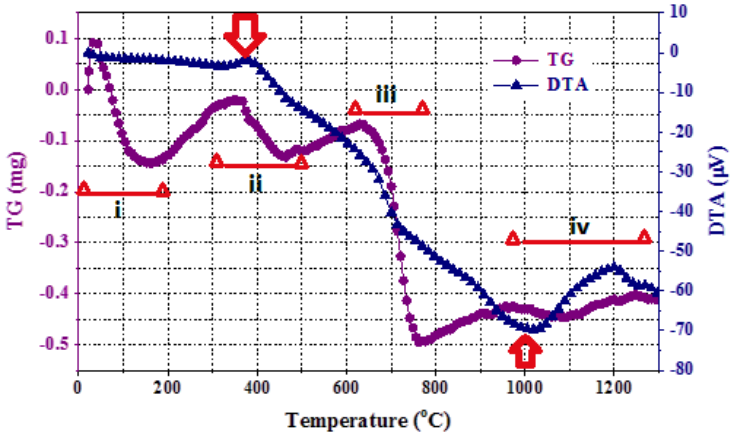


**Figure 2.** TGA and DTA curves of dried gel.

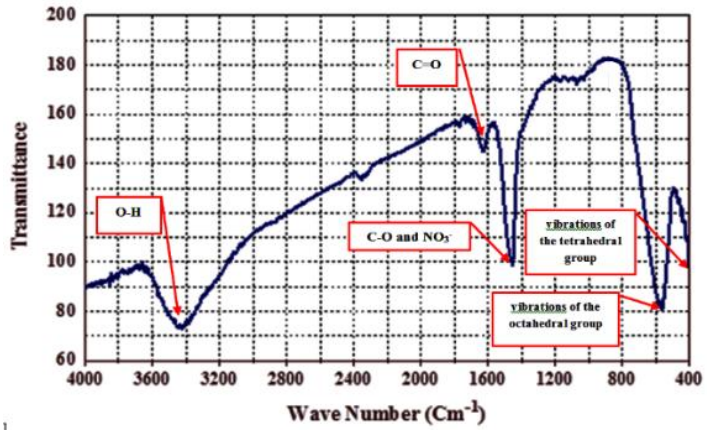


**Figure 3.** Infrared spectroscopy results of the dried gel.

### 3.2. FTIR ANALYSIS

The FTIR spectroscopy is a very useful technique to deduce the structural investigation and redistribution of cations between octahedral and tetrahedral sites of hexaferrite structure [10]. FTIR spectrum data for the respective sites are analyzed in the range of 4000-400 $cm^{-1}$ and shown in Figure 3. The broad absorption band at 3415 $cm^{-1}$ corresponds to the hydroxyl (-OH) group stretching vibrations due to the water presence, bands at about 1620 and 1450 $cm^{-1}$, corresponding to the carboxyl

group and $NO_3^-$ ion, respectively. The band at about 830 $cm^{-1}$ also corresponds to the $NO_3^-$ ion. The vibration bands present in the spectra at 563 $cm^{-1}$ and 418 $cm^{-1}$ are the common features of all the ferrites [11, 12]. The tetrahedral cations must be of higher valence than the octahedral cation, so here the absorption band at 590 $cm^{-1}$ is assigned to the stretching vibrations of the octahedral group and the band at 433 $cm^{-1}$ is attributed to the stretching vibrations of the tetrahedral group [13].

### 3.3. XRD ANALYSIS

X-ray diffraction patterns of the calcined powders at 800, 900, 950, 1000 and 1050 ˚C for 3hrs are shown in Figure 4. The XRD patterns of samples heat treated at temperatures (800-950 ˚C) were complex in nature and showed many peaks due to the presence of various phases like $Fe_3O_4$, $ZnFe_2O_4$, $MgFe_2O_4$, $CoFe_2O_4$ and $SrFe_{12}O_{19}$. The characteristic peaks of $Sr_2Co_2Fe_{12}O_{22}$ (PDF 82-0472) phase appeared when the sample was calcined at 950˚C, but the crystallinity was not quite high and some other phases still existed.

There was no change in the XRD patterns except one peak which was due to the formation of $Co_2Y$ at the temperatures of (1000~1050 ˚C). The single phase Y-type hexaferrite was successfully prepared at 1000 ˚C. Calcination at 1050 ˚C led to an increase in diffraction peak intensity and a decrease in peak full width at half maximum (FWHM), which indicated more complete crystallization of the samples with the calcination temperature [13, 14].

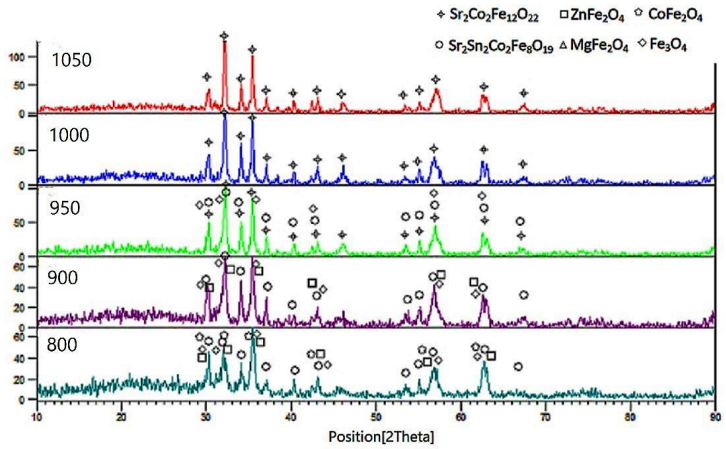


**Figure 4.** X-ray diffraction pattern of calcined powders at 800, 900, 950, 1000 and 1050 ˚C for 3hrs.

The main peaks of Y-type strontium hexaferrite ($Sr_2Co_2Fe_{12}O_{22}$) were appeared at 2θ = 30.26, 32.19, 34.12, 35.45, 37.08, 40.31, 43.08, 46.13, 53.30, 55.05, 56.74, 62.53, 63.08, 67.58 and 76.49 revealing typical hexagonal plans of (1 1 0), (1 0 13), (1 1 6), (0 1 14), (1 1 9), (2 0 5), (0 2 7), (0 1 10), (2 0 14), (1 2 11), (2 1 13), (1 2 14), (1 0 28), (4 0 7).

The calculated values of lattice constants, crystallite size and unit cell volume are given in Table 1. The observed values of the lattice parameters (a=5.98 Å, c=42.63 Å) and unit cell volume (1324.09 $Å^3$) are very close to the reported values for Y-type hexagonal ferrites [4].

**TABLE 1.** Calculated value of lattice parameters (a and c), cell volume (V), c/a ratio and crystallite size (D) for $Sr_2Co_{1.7}Mg_{0.3}Fe_{11.2}Sn_{0.4}Zn_{0.4}O_{22}$ hexaferrites at 1000 °C.

| Temp. (°C) | a (Å) | c (Å) | c/a ratio | V ($Å^3$) | D (nm) |
|---|---|---|---|---|---|
| 1000 | 5.987 | 42.609 | 7.122 | 1324.092 | 44.607 |

### 3.4. MICROSTRUCTURE ANALYSIS

Microstructure of the as-burnt powder and calcined powders at 900 and 1000 ˚C is shown in Figure 5. It was observed that as-burnt powders contain well distributed simple metal oxide particles in a range of 60-70 nm, which is the key factor in producing final product at lower temperature compared with common solid reaction synthesis [10]. It was observed that well defined hexagonal plates with particle sizes between 90 and 210 nm were formed at low temperature (say 1000 ˚C). It is well known that the M-type ferrite has also exhibited hexagonal shapes, but no hexagonal shaped particles were observed in the FESEM when the samples were heat treated at 900 ˚C (Figure 5(b)), therefore, the hexagonal plates appeared at 1000 ˚C were definitely due to the presence of $Co_2Y$ hexaferrite. The grain sizes estimated from FESEM images is in the range of 82-210 nm considered to be in nanosized range and in

comparison to the other studies, are very fine and homogenous particles [4, 17, 18].

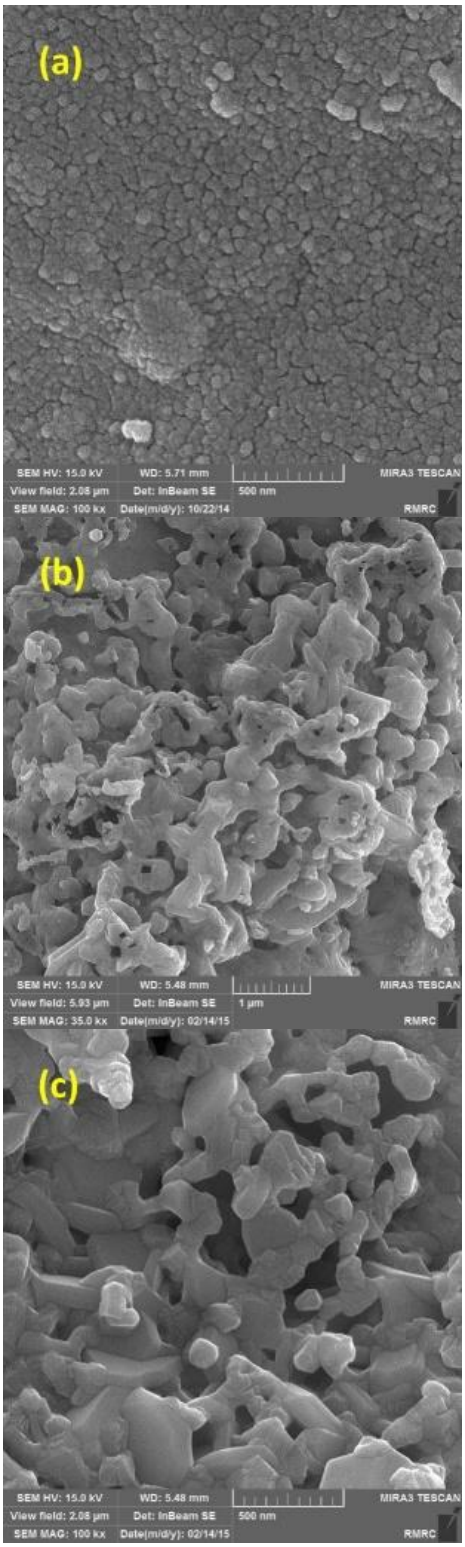


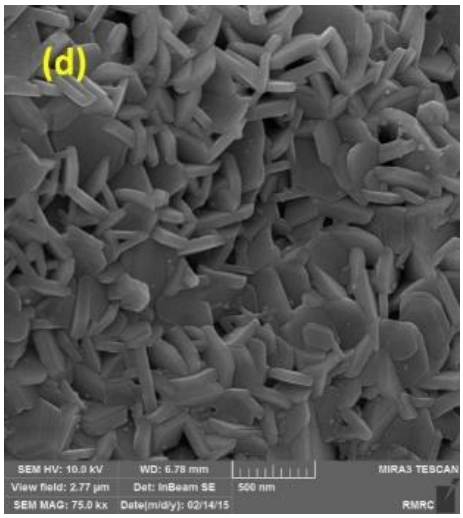


**Figure 5.** FESEM images of the powders of (a) as-burnt, (b) calcined at 900, (c) 950 and (d) 1000 ˚C.

### 3.5. MAGNETIC PROPERTIES

Figure 6 shows the magnetization curve of a selected sample heat treated at 1000 ˚C. The magnetic properties such as saturation magnetization ($M_s$), remanance ($M_r$) and coercivity ($H_c$) are calculated from the hysteresis loops and the results are listed in Table 2. The saturation magnetization ($M_s$) and the coercivity ($H_c$) of the samples were in the range of 28.34–48.47 emu/g and 637-1108 Oe, respectively, depending on the heat treatment temperature (950~1000 ˚C).

The samples heat treated at 1000 ˚C showed maximum $M_s$ (48.47 emu/g) and $H_c$ (637 Oe). The weak saturation magnetization at 950 ˚C is because of the formation of $SrFe_{12}O_{19}$, spinel ferrite and hematite as intermediate, which hematite well known to exhibit the lowest saturation magnetization and large coercivity [14, 7]. The $M_s$ of the samples wereincreased to 48.47 emu/g and the Hc decreased to 637 Oe, when the formation of single Y-type hexaferrite took place, especially when the sample was heat treated at 1000 ˚C for 3hrs. $H_c$ of sample synthesized at 1000 ˚C for 3hrs was lower than that from an earlier report [17] for Y-type hexagonal ferrites with formula of $Sr_2Co_2Fe_{12}O_{22}$.

### 4. CONCLUSION

Nanoparticles of $Sr_2Co_{1.7}Mg_{0.3}Fe_{11.2}Sn_{0.4}Zn_{0.4}O_{22}$ ferrites were synthesized successfully by the sol-gel auto combustion method. The Results of XRD, FESEM and DTA analysis indicated that single phase Y-type hexaferrite powders with uniform hexagonal plate structure were produced at the calcination temperature

above 1000 ˚C as compared to that of conventional solid state reaction method (1100 ˚C)

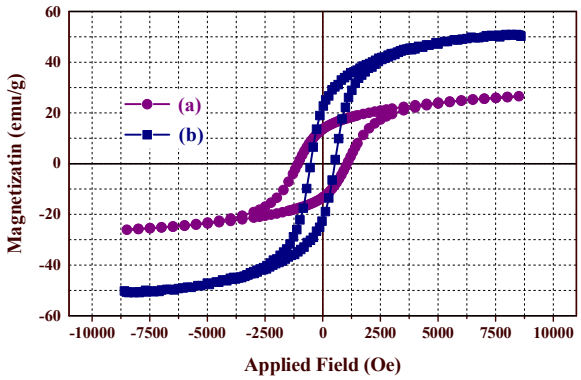


**Figure 6.** Magnetic hysteresis loops of calcined samples at (a) 950 and (b) 1000 ˚C.

**TABLE 2.** The measured values of the saturation magnetization (Ms), remanent magnetization (Mr), and coercivity (Hc).

| Temperature (°C) | $M_s$ (emu/g) | $M_r$ (emu/g) | $H_c$ (Oe) |
|---|---|---|---|
| 950 | 28.34 | 13.87 | 1108 |
| 1000 | 48.47 | 20.44 | 637.26 |

The grain size is in the range of 82-210 nm and in comparison with other studies is very fine and has homogenous particles. The saturation magnetization increased from 28.34 to 48.47 emu/g by increasing heat treatment temperature above 950 ˚C, while the coercivity decreased from1108 to 637 Oe; moreover, low value of coercivity makes these ferrites potential candidates for security, switching, sensing and high frequency applications and is also favorable for electromagnetic (EM) materials.

## ACKNOWLEDGEMENT

The authors would like to thank the Iranian Nanotechnology Initiative Council for providing us with financial support in this project.

## REFERENCES

A. Mali, A. Ataie, "Influence of the metal nitrates to citric acid molar ratio on the combustion process and phase constitution of barium hexaferrite particles prepared by sol–gel combustion method," ***Ceramics International 30*** (2004) 1979–1983.

4. M. Ahmad, M. Ahmad, I. Ali, W. Ahmad, G. Mustafa, M. Niaz Akhtara, A. Ali, "Temperature dependent structural and magnetic behavior of Y-type hexagonal ferrites synthesized by sol-gel autocombustion," ***Journal of Alloys and Compounds***, 2015.
5. D.H. Bobade, S.M. Rathod, Mahesh-kumar L.Mane, "Sol–gel auto-combustion synthesis,structural and enhanced magnetic properties of $Ni_2Y$ substituted nanocrys-talline Mg–Zn spinel ferrite," ***Physica***, vol. 407, p. 3700–3704, 2012.
6. Asmat Elahi, Mukhtar Ahmad, Ihsan Ali, M.U. Rana., "Preparation and properties of sol–gel synthesized Mg substituted $Ni_2Y$ hexagonal ferrites," ***Ceramics International*** 39 (2013) 983–990.
7. H.C. Fang, Z. Yang, , C.K. Ong, Y. Li, C.S. Wang, "Preparation and magnetic properties of (Zn-Sn) substituted barium hexaferrite nanoparticles for magnetic re-cording," ***Journal of Magnetism and Magnetic Materials***, pp. 187 (1998) 129-135.
8. C. Zhang, J. Shi, X. Yang, L. De, X. Wang, "Effects of cal-cination temperature and solution pH value on the structural and magnetic properties of $Ba_2Co_2Fe_{12}O_{22}$ ferrite via EDTA-complexing process," ***Journal of Materials Chemistry and Physics***, 123 (2010) 551-556.
9. L.I. Liyanage, S. Kim, Y.K. Hong, J.H. Park, S.C. Erwin, "Theory of magnetic enhancement in strontium hexaferrite through Zn–Sn pair substitution", ***Journal of Magnetism and Magnetic Materials***, 348 (2013) 75–81.
10. G. Mendoza-Suarez, L.P. Rivas-Vazquez, J.C. Corral-Huacuz, A.F. Fuentes, J.I. Escalante-Garcıa, "Magnetic properties and microstructure of $BaFe_{11.6-2x}Ti_xM_xO_{19}$ (M=Co, Zn, Sn) compounds," ***Physica B*** 339 (2003) 110–118.
11. M. Javed Iqbal, B. ul-Ain, "Synthesis and study of physical properties of $Zr^{4+}$–$Co^{2+}$ co-doped barium hexagonal ferrites", ***Journal of Materials Science and Engineering,*** B 164 (2009) 6–11.
12. I. Ali, A. Shakoor, M.U. Islam, M. Saeed, M. Naeem Ashiq, M.S. Awan, "Synthesis and characterization of hexagonal ferrite $Co_2Sr_2Fe_{12}O_{22}$ with doped polypyrrole composites", ***Current Applied Physics*** 13 (2013) 1090-1095.
13. G. Murtaza , R. Ahmad , T. Hussain , R. Ayub , Irshad Ali , Muhammad Azhar Khan , Majid Niaz Akhtar , "Structural and magnetic properties of Nd–Mn substituted Y-type hexaferrites synthesized by microemulsion method," ***Journal of Alloys and Compounds*** 602 (2014) 122–129.
14. N. Chand Pramanik, T. Fujii, M. Nakanishi, J. Takada, S. Seok, "The effect of heat treatment temper-ature on the microstructure and magnetic properties of $Ba_2Co_2Fe_{12}O_{22}$ ($Co_2Y$) prepared by sol–gel method," ***Materials Letters***, 60 (2006) 2718–2722.
15. G. Reza Gordania, A. Ghasemi, A. Saidia, "Enhanced magnetic properties of substituted Sr-hexaferrite nanoparticles synthesized by co-precipitation method", ***Ceramics International*** 40 (2014) 4945-4952.
16. A. Davoodi, B. Hashemi, "Magnetic properties of Sn–Mg substituted strontium hexaferrite nanoparticles synthesized via co-precipitation method," ***Journal of Alloys and Compounds*** 509 (2011) 5893–5896.
17. S.H. Mahmoodad, F.S. Jaradat, A.F. Lehlooh, A. Hammoudeh, "Structural properties and hyperfine interactions in Co–Zn Y-type hexaferrites prepared by sol–gel method," ***Ceramics International***, 40 (2014) 5231–5236.
18. Y. Alizad Farzin, O. Mirzaee, A. Ghasemi, "Influence of Mg and Ni substitution on structural,micro structural and magnetic properties of $Sr_2Co_{2-x}Mg_{x/2}Ni_{x/2}Fe_{12}O_{22}$ ($Co_2Y$) hexaferrite", ***Journal of Magnetism and Magnetic Materials,*** 371 (2014) 14–19.
19. G. Albanese, "Recent advances in hexagonal ferrites by the use of nuclear spectroscopic methods", ***Colloque CI, Tome*** 38 (1977) Cl-85.